

# OmniV2V: Versatile Video Generation and Editing via Dynamic Content Manipulation

Sen Liang<sup>1,2\*</sup> Zhentao Yu<sup>2</sup> Zhengguang Zhou<sup>2</sup> Teng Hu<sup>2</sup> Yi Chen<sup>2</sup> Hongmei Wang<sup>2</sup>  
 Qin Lin<sup>2</sup> Yuan Zhou<sup>2</sup> Xin Li<sup>1</sup> Qinglin Lu<sup>2†</sup> Zhibo Chen<sup>1†</sup>  
<sup>1</sup>University of Science and Technology of China <sup>2</sup>Tencent Hunyuan

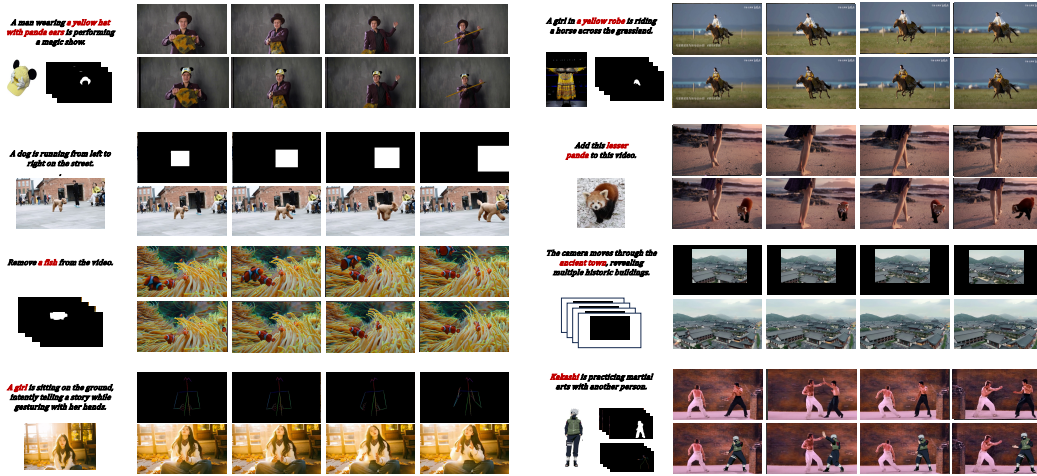


Figure 1: **OmniV2V comprehensive capability demonstration.** We showcase the excellent generation and editing results of OmniV2V, with the original input and the generated videos for each task displayed in the figure.

## Abstract

The emergence of Diffusion Transformers (DiT) has brought significant advancements to video generation, especially in text-to-video and image-to-video tasks. Although video generation is widely applied in various fields, most existing models are limited to single scenarios and cannot perform diverse video generation and editing through dynamic content manipulation. We propose OmniV2V, a video model capable of generating and editing videos across different scenarios based on various operations, including: object movement, object addition, mask-guided video edit, try-on, inpainting, outpainting, human animation, and controllable character video synthesis. We explore a unified dynamic content manipulation injection module, which effectively integrates the requirements of the above tasks. In addition, we design a visual-text instruction module based on LLaVA, enabling the model to effectively understand the correspondence between visual content and instructions. Furthermore, we build a comprehensive multi-task data processing system. Since there is data overlap among various tasks, this system can efficiently provide data augmentation. Using this system, we construct a multi-type, multi-scenario OmniV2V dataset and its corresponding OmniV2V-Test benchmark. Extensive experiments show that OmniV2V works as well as, and sometimes better than, the best existing open-source and commercial models for many video generation and editing tasks. Our project is available at OmniV2V.

\*Work done during the internship at Tencent.

†Corresponding author. qinglinlu@tencent.com, chenzhibo@ustc.edu.cn

# 1 Introduction

In recent years, Diffusion Transformers (DiT) has led to significant advancements in video generation models. Text-to-video and image-to-video generation [2, 63, 4, 5, 14, 61, 15, 49, 16, 6, 51, 45, 30, 47, 32] have attracted increasing attention as they approach the threshold of practical application. In addition, downstream tasks based on these pre-trained models have become increasingly diverse, such as object movement, object addition, mask-guided video edit, try-on, human animation, controllable character video synthesis, inpainting, and outpainting. These tasks involve different content inputs, reflecting the dynamic and complex nature of video generation and editing.

Current video generation models perform well on specific tasks, but each new task typically requires dedicated modules and fine-tuning. For example, in character image animation, methods like Animate Anyone [18] use ReferenceNet [18] to fit the reference character, while pose is driven by adding it to the noise. For object addition, Get in Video [65] uses a T5 encoder [7] to input instructions and compresses the original video and reference image through a 3D VAE. In try-on task, methods such as Tunnel Try-on [52] and Stableviton [26] use ReferenceNet or ControlNet [56] to inject clothing information, performing clothing replacement by concatenating the source video, mask video, and other information along the channel dimension. Although these approaches achieve impressive results, their complex structures and lack of interoperability lead to significant waste of computational and data resources. We observe that leveraging commonalities among tasks can help models better understand and perform across tasks. For example, in mask-guided video editing, the role of text is often overlooked, either the text branch is removed or only captions are encoded, largely ignoring the relationship between text and image. In object movement task, boundingbox information dominates, and textual information is neglected.

To address the high deployment and training costs associated with task-specific video generation models, we propose **OmniV2V, a unified framework capable of both video generation and editing** according to diverse user operations. Building on the mainstream MM-DiT architecture, we adopt HunyuanVideo [28] as our backbone to maximize model capacity and performance. To enable flexible and effective handling of various tasks, we first introduce a unified **dynamic content manipulation injection module**. This module integrates all dynamic content operation inputs such as reference images, background videos, pose videos, and mask videos into a single framework, leveraging multi-modal information. To distinguish between different visual modalities across tasks, we employ a dynamic routing strategy that adaptively adjusts model inputs, allowing the model to discern which content should be preserved and which should be modified. Furthermore, we design a **visual-text instruction module** based on LLaVA [35], enabling the model to better understand and align visual content with textual instructions. Unlike HunyuanVideo, which only uses LLaVA for text understanding and does not establish explicit connections between text and visual content, our approach ensures that the model can accurately associate reference images with textual concepts in the caption. This alignment is crucial for tasks involving reference images, as it allows the reference character to act according to the given instructions.

To construct comprehensive datasets for various tasks, we utilize a multi-task data processing system and leverage various open-source tools in combination to efficiently filter and select high-quality data. To comprehensively evaluate our model’s performance on different tasks, we build task-specific benchmarks. By comparing with existing open-source and commercial methods, it demonstrates the strong competitiveness of our model. Extensive experiments show that our design can effectively unify various video generation and editing tasks, significantly improving video dynamics and reference consistency. In summary, our contributions can be summarized as follows:

- We propose **OmniV2V**, a unified video generation and editing framework that supports a wide range of user operations, including object addition and replacement, video inpainting and outpainting, pose-guided generation, and more.
- We introduce a **unified dynamic content manipulation injection module** that flexibly integrates multi-modal inputs (e.g., reference images, background videos, and pose videos) and employs a dynamic routing strategy to distinguish and process different visual modalities.
- We design a **visual-text instruction module** based on LLaVA, enabling the model to effectively align and understand the correspondence between visual content and textual instructions for more accurate and controllable video editing.



- We construct **comprehensive multi-task datasets** and **task-specific benchmarks** using a multi-task data processing system and open-source tools, facilitating robust evaluation and demonstrating the competitiveness of our approach against existing methods.

## 2 Related work

### 2.1 Video Generation Model

Recent advancements in video generation have been significantly propelled by diffusion models, which have evolved from static image synthesis [44, 31, 29] to video generation [17, 57]. The field has seen substantial progress with the development of large-scale frameworks [36, 55, 27, 48, 63], which demonstrate unprecedented high-quality content creation and a diverse array of generated results through extensive training on video-text pairs. However, existing methods primarily focus on either text-guided video generation [33] or video generation based on a single reference image [13, 53]. These approaches often struggle to provide fine-grained control over the generated content and precise concept-driven editing, a limitation that persists despite advancements in multi-condition control. While pioneering work such as VACE 1.3B [23] enables multi-condition capabilities through multi-modal modeling, it fails to maintain identity consistency due to the excessive number of training tasks. In this study, we focus on video editing and aim to enhance the consistency of characters or objects through sophisticated data processing and the design of a video injection model.

### 2.2 Video Editing

Using video and masked video as default inputs, many different scenarios can be achieved, such as virtual try-on, inpainting, outpainting, object addition, and object replacement. By adding additional pose references, character animation can also be achieved.

**Human Animation.** Character animation based on diffusion models has made significant progress in generating appearance consistent and motion stable animations. Animate Anyone [18] proposes ReferenceNet to inject character appearance into a symmetric UNet and employs a pose guider to drive the reference pose. Furthermore, to interact characters with real-world environments, Animate Anyone 2 [19] utilizes 3D VAE to encode the environment and object to achieve seamless character-environment integration. For the same purpose, Mimo [37] first encodes video scenes and floating occlusions with VAE and extracts identity and motion using ID encoders and a pose encoder, separately. Mimicmotion [59] adopts an auxiliary loss on high-confidence regions of body parts, achieving superior portrait frame quality, especially in the hand regions. These methods require pose as a condition and cannot be generalized well to other objects.

**Video Inpainting.** Video inpainting aims to remove certain areas of the video and keep it consistent with the unchanged content. Propainter [62] incorporates enhanced dual-domain propagation and an efficient mask-guided sparse video Transformer for video inpainting. Based on text-to-image models, CoCoCo [66] introduces trainable temporal layers to adapt to video inpainting tasks. VideoPainter [3] implements a dual-branch architecture that leverages an efficient context encoder with any pre-trained DiT, decoupling video inpainting into background preservation and foreground generation.

**Video Virtual Try-on.** The objective of virtual try-on is to transfer the given garment to a target person in the video. MV-TON [60] proposes a two-stage framework to overcome the difficulty of dealing with a large variety of poses and improves the details through a memory refinement operation in video virtual try-on. Clothformer [22] obtains a temporally consistent warp sequence using a tracking strategy based on optical flow and ridge regression, and uses a dual-stream transformer to process the warped input sequences. ViViD [12] introduces a UNet-like encoder to preserve garment consistency and collects a large virtual try-on dataset to improve generation quality.

**Video Addition.** Video object insertion aims to insert a user-provided reference object into certain areas of the target video while maintaining the consistency of unedited regions. VideoAnyDoor [46] designs an end-to-end zero-shot video insertion framework that precisely modifies both content and motion according to user-provided instructions while keeping the unedited content unchanged. GetInVideo [65] adopts a diffusion transformer architecture with 3D full attention to process reference images, condition videos, and masks simultaneously, maintaining temporal coherence, preserving visual identity, and ensuring natural scene interactions when integrating reference objects into videos.

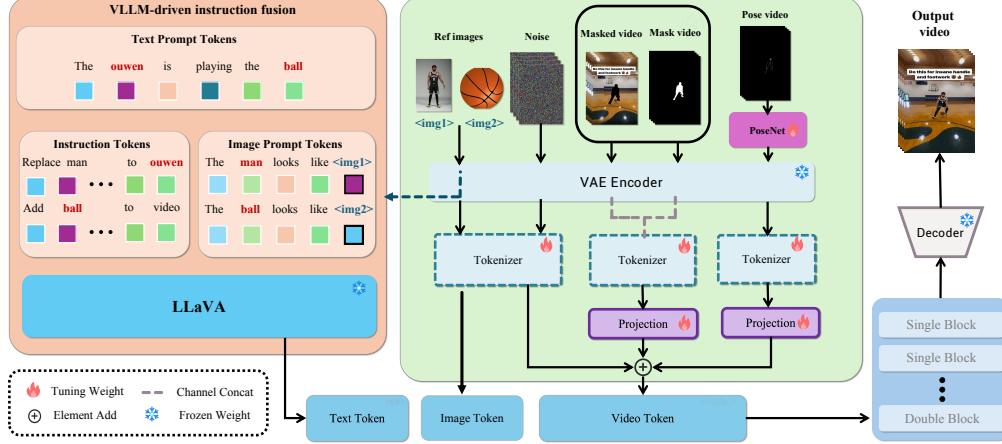


Figure 2: The framework of OmniV2V. It consists of two main modules: a unified information injection module for integrating task requirements and a visual-text instruction module for understanding visual-instruction correspondence.

### 3 Methods

We propose a unified video editing approach, **OmniV2V**, which supports various primary control signals as input to generate corresponding videos using textual information. Specifically, our method allows for image, video, mask video, and pose video as conditional inputs to produce video content specified by text. This enables key video editing tasks such as object replacement, object addition, instruction-based editing, video inpainting, outpainting, pose-driven editing, and video face swapping. In detail, we introduce a unified dynamic content manipulation injection module that categorizes conditional inputs into image signals, mask signals, and pose signals, achieving decoupled processing and conditional fusion of these three types. Through a dynamic conditional training strategy, the model is capable of understanding individual signals while also integrating multiple signals, thereby enhancing the control capability of each signal through multi-signal comprehension. Additionally, we propose an instruction-based editing method based on LLaVA, which leverages a multimodal understanding model to effectively interpret human instructions while integrating image signal comprehension, thus enabling the conditional injection from text-image signals to video generation.

#### 3.1 Unified dynamic content manipulation injection

We first categorize the conditional signals into three components: image conditions ( $I$ ), mask conditions, and pose conditions ( $V_P$ ). The mask conditions can be further subdivided into the masked source video ( $V_S$ ), which is a video with certain regions masked, and the mask video ( $V_M$ ), which consists of a sequence of binary masks. To enable decoupled processing of these three types of signals, we design a multimodal conditional fusion module. Specifically, the masked source video, mask video, and condition image are treated as the same modality and are encoded using a pretrained 3D-VAE encoder to extract their respective video and image features.

**Latent-Fusion Video Tokenizer.** Since the masked source video and mask video contain overlapping information—where the masks in the mask video correspond to the masked regions in the source video—we employ a latent fusion tokenizer to merge these two streams of tokens into a single set, thereby effectively compressing the conditional information. Concretely, the 3D-VAE encoder encodes both videos from the RGB channel into 16-dimensional latent representations. These features are then concatenated to form a 32-dimensional feature vector. The original tokenizer in the pretrained HunyuanVideo model consists of a 3D convolutional network that maps the 16-dimensional features into a sequence of tokens. To leverage the robust tokenization capabilities of the pretrained tokenizer, our latent fusion tokenizer inherits its weights and pads zeros in the 3D convolutional layer to accommodate the 32-dimensional input. This process yields a set of fused tokens  $T_M$  that integrate information from both the source and mask videos.

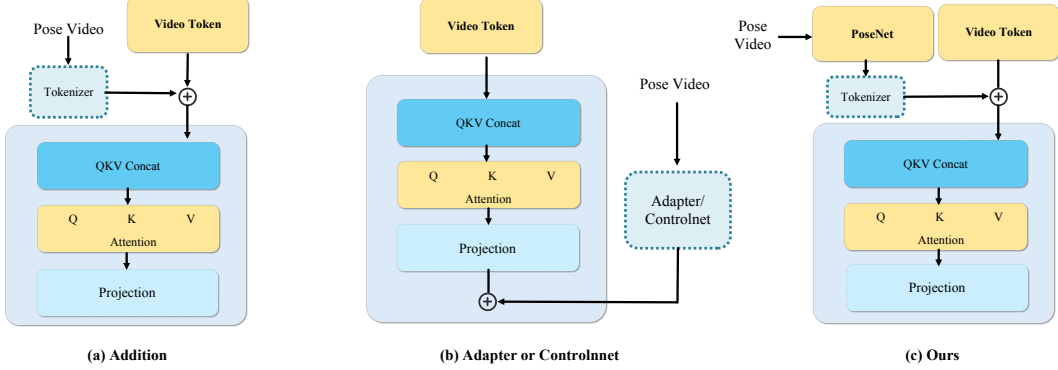


Figure 3: Three types of strategies for injecting pose information.

**PoseNet.** Effectively inputting pose-guided information into the model poses a challenge. Since our model is built on the HunyuanVideo framework—a video generation architecture based on MM-DiT—we considered two commonly used conditional injection strategies from MM-DiT: (1) Token Addition (as shown in figure 3(a)): This involves encoding the pose video into pose tokens using a tokenizer and then adding them element-wise to the video tokens. (2) ControlNet-based Method (as shown in figure 3(b)): This involves extracting pose information through an additional adapter network and injecting it between the layers of the HunyuanVideo model. However, both methods were initially designed for image generation and exhibit significant limitations when applied to video generation tasks. In the Token Add approach, we found that pose information tends to leave residual artifacts in the generated video, a problem that requires extended training time to mitigate. As for the ControlNet method, since pose video inherently contains relatively sparse information and ControlNet’s structure is complex with a large number of parameters, the model struggles to effectively learn the crucial pose-guided signals, thereby affecting the injection effectiveness.

**Token Fusion.** After obtaining the feature-aligned video tokens  $T_M$  from the masked source and mask videos, the pose tokens  $T_P$ , and the noisy latent tokens  $T_V$ , a key challenge is to establish effective correlations among them so that the noisy latent tokens can adequately incorporate the conditional information. Previous image-editing approaches often utilize adapter-based methods to inject conditions into the latent space. However, for the MMDiT-based HunyuanVideo model, the large parameter count, high-dimensional feature space, and long video token sequences make it difficult for a newly introduced module to map the conditional features into the latent space efficiently. To address this, we propose a more efficient video condition injection mechanism that merges all tokens. Specifically, we first apply a fully connected (FC) layer to the two sets of condition tokens, mapping them into the latent space of the video tokens. With the aligned video, mask, and pose tokens, we directly sum them to form a new set of tokens. This approach enables effective injection of conditional information into the video tokens. Furthermore, the learnable FC layer preceding the token addition allows the model to selectively retain or discard features, ensuring that only the most salient conditional information is incorporated. Ultimately, this results in fused video tokens that are well-integrated with the relevant condition information.

**Dynamic Content Manipulation Injection.** Given the presence of multiple video conditions in the model, it is not always necessary to utilize all conditions during editing. For example, in some cases, the pose video or mask video alone may suffice to generate the output, while in others, the mask video may need to be combined with the source video. To facilitate flexible video editing with arbitrary combinations of input conditions, we propose a dynamic content manipulation injection strategy. During training, we randomly set some of the conditional inputs to empty, enabling the model to learn to handle various combinations of conditional information. This unified training approach not only enhances the model’s ability to process different sets of conditions but also improves its performance when editing based on a single condition, thereby significantly boosting its overall editing capabilities.

### 3.2 VLLM-driven instruction-based editing

In previous video editing methods, the model typically overlooks the text prompt, resulting in output videos determined solely by the input masked source video and mask video. However, the absence

of a text prompt significantly limits the controllability of these methods, as it prevents users from precisely specify the desired editing outcomes. To address this limitation, we propose a VLLM-driven, instruction-based editing module that leverages the strong multimodal understanding capabilities of the pretrained LLaVA model to enable instruction-guided editing. Specifically, we decompose the text tokens in LLaVA into three components: (1) *instruction tokens*, which encode the user-provided editing instruction (i.e., what to edit); (2) *text prompt tokens*, which describe the content of the video the user wishes to generate; and (3) *image prompt tokens*, which incorporate a target image into the LLaVA text space. For example, to add a cat to a source video depicting a beach scene, the instruction prompt could be “Add a cat to the video,” the text prompt might be “A cat is playing on the beach,” and the image prompt could be “The cat looks like <image>.” To clearly separate these three sets of tokens, we follow HunyuanCustom [20] and insert a <SEP> token between them. The concatenated tokens are then input into the LLaVA model, which, through its autoregressive multimodal modeling capability, establishes correlations among the three sets of tokens to produce output text tokens.

Since the CLIP image encoder in LLaVA primarily captures high-level semantic features and may lose fine-grained image details, we additionally employ a 3D-VAE to encode the image, mapping it into the latent space while preserving detailed information. To effectively inject these image tokens into the model, we position the image along the temporal axis of the video tokens, specifically placing it before the first frame of the video tokens. Given that the pretrained video model possesses strong temporal modeling capabilities, the information from the image can be efficiently integrated into the video tokens via temporal modeling. In particular, the base video generation model (HunyuanVideo) utilizes 3D-RoPE to model the relative positions of video tokens, where the pixel at the  $t$ -th frame and spatial location  $(i, j)$  is assigned a RoPE index  $(t, i, j)$ . For the image tokens, we assign them to the  $-1$ -th frame (i.e., preceding the first video frame). Furthermore, to prevent the model from simply copy-pasting the image onto the video, we introduce a spatial shift as follows:

$$\text{Pos}(i, j) = \text{RoPE}(-1, i + w, j + h), \quad (1)$$

where  $w$  and  $h$  denote the width and height of the video, respectively.

## 4 Experiment

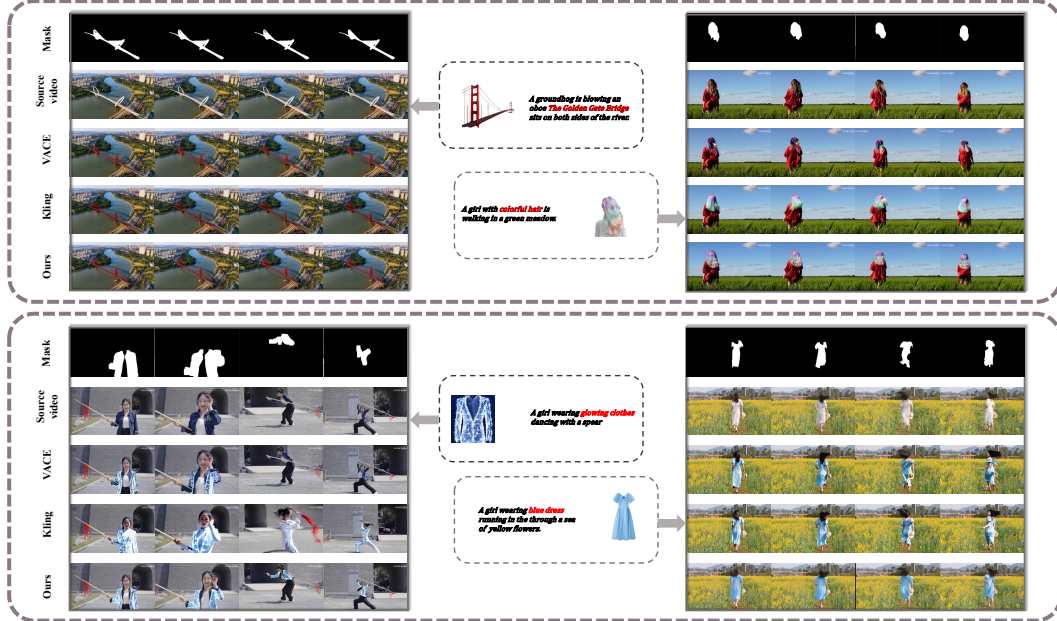


Figure 4: Qualitative of comparison on the wild dataset.

### 4.1 Experiment Settings

**Implementation Details.** We adopted a phased strategy for the training process. We first train the mask-guided video edit task, which easily allows the model to extend to object movement, inpainting,

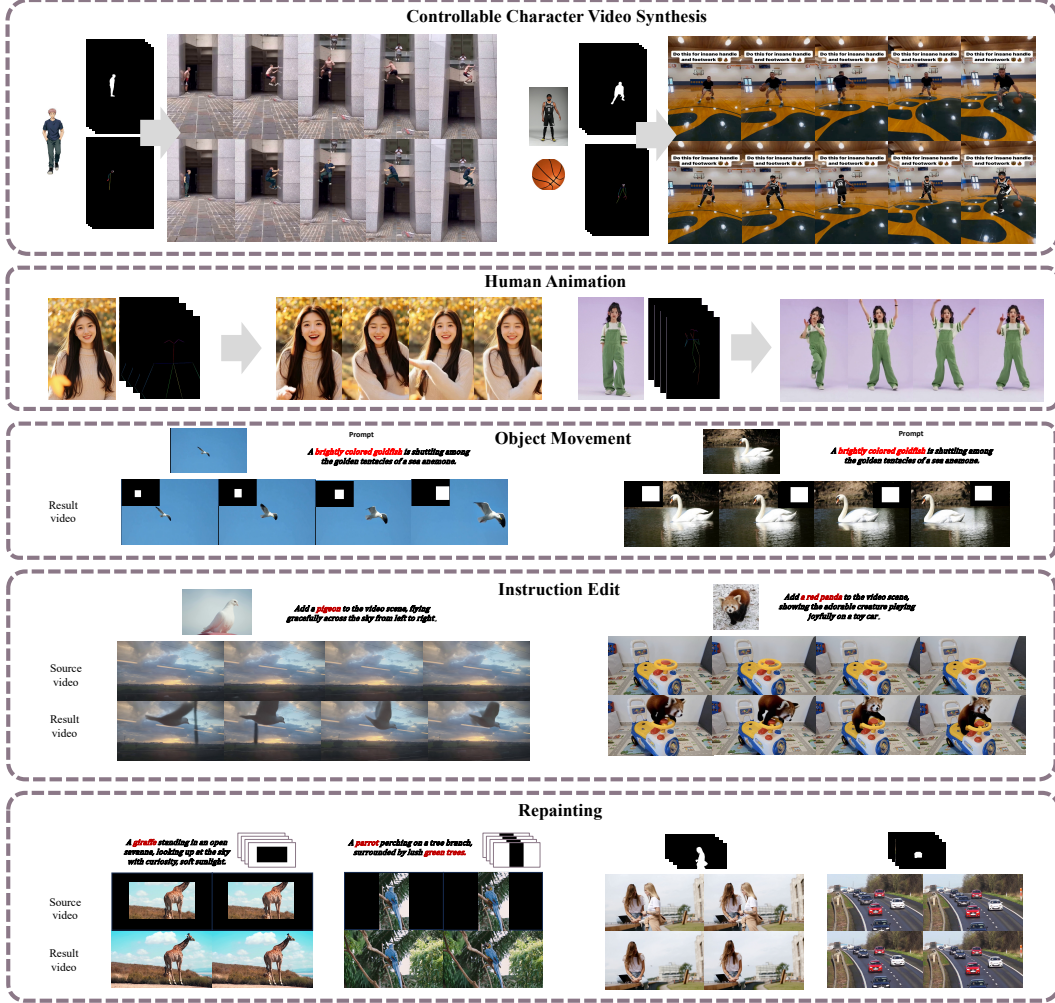


Figure 5: Visualization of videos generated by OmniV2V on the wild dataset.

and outpainting tasks. The introduction of mask information enables the model to effectively learn the ability to generate context in the spatiotemporal dimensions. After extending the tasks to object movement, inpainting, and outpainting, the model has already learned a good correspondence between objects and text, which significantly reduces the difficulty of training the instruction edit task in the second phase. Finally, since the aforementioned edit tasks have already learned the correspondence between characters and masks, extending it to the controllable character video synthesis task only requires fitting the pose information. This training process greatly reduces the time cost of training individual tasks and enhances the model’s performance.

**Datasets.** To obtain the high-quality data required, we used PySceneDetect [41] to segment transition videos into single-shot videos, Textbpn-Plus-Plus [58] to filter out videos with excessive subtitles, and the Koala-36M [50] model to further refine our data selection. To extract the objects in the videos, we first used the Qwen-7B [1] model to extract all object IDs in the videos. For portrait data, we used ArcFace [8] to locate faces to ensure detection accuracy and filtered out the IDs that appeared in the most frames. Based on keywords, we used Grounding Sam2 [43] to extract object masks and bounding boxes, discarding objects that were excessively large or small. Due to size differences between objects, we randomly expanded the masks in all four directions to mitigate the issue of overly restrictive masks.

For different tasks, we need to perform customized data operations: (1) For the inpainting task, we randomly inpaint the video based on different object masks. For the outpainting task, we randomly



Table 1: Quantitative comparisons with mask-guided video edit baselines and controllable character video synthesis baselines.

Method	Face-sim $\uparrow$	DINO-sim $\uparrow$	CLIP-B $\uparrow$	CLIP-L $\uparrow$	FVD $\downarrow$	Temporal $\uparrow$	DD $\uparrow$	SC $\uparrow$	MD $\uparrow$	VQ $\uparrow$
VACE 1.3B	0.587	0.576	0.330	0.274	1171.42	0.966	0.52	5.66	4.32	6.66
Kling 1.6	0.34	0.58	<b>0.346</b>	<b>0.276</b>	1049.70	0.93	0.64	3.33	8.64	7.32
Ours	<b>0.614</b>	<b>0.59</b>	0.328	0.274	<b>900.35</b>	<b>0.967</b>	<b>0.69</b>	<b>8.67</b>	<b>8.77</b>	<b>8.56</b>
Mimo	0.446	<b>0.562</b>	–	–	1088.56	0.802	0.55	3.33	5.00	7.66
Ours	<b>0.593</b>	0.553	–	–	<b>862.21</b>	<b>0.856</b>	<b>0.64</b>	<b>8.23</b>	<b>7.65</b>	<b>8.55</b>

crop the original video and use the bounding box of the crop as our conditional input. (2) For the addition task in the instruction edit task, we can effectively use the before-and-after data from the inpainting task as pairs. For the swap task in the instruction edit task, we can effectively use the trained mask-guided video edit model to generate pairs. (3) For the Character Animation task and the controllable character video synthesis task, we used DWpose [54] to extract the actions of characters in the videos. Due to significant differences in body types between characters, we also performed body type data augmentation on the DWpose data.

Furthermore, due to the absence of a publicly available unified multi-task dataset, we have developed the OmniV2V-Test dataset. This test set comprises 100 pairs for each task, encompassing a variety of species, styles, and more. The diverse data distribution within the testset is designed to thoroughly evaluate the capabilities of various models.

**Evaluation Metrics.** To evaluate the model performance, we use the following metrics to measure the object consistency in videos, text-video alignment, and video generation quality: **ID consistency.** We employ RetinaFace [9] and Arcface [8] to detect and extract the embedding of the reference face and each frames of generation video, and then compute the average cosine similarity between them. **Object similarity.** First, we detect each frame and get the segment result of human using YOLOv11 [25], and then compute the similarity of the DINO-v2 [39] feature between the reference and results. **Text-video alignment.** We employ CLIP-B [42] to evaluate the alignment between the given text prompt and the corresponding generated videos. **Temporal consistency.** Following VBench [21], we utilize the CLIP-B [42] model to calculate the similarity between each frame and its adjacent frames, as well as the first frame, to assess the temporal consistency of the video. **Dynamic degree.** The dynamic degree is used to measure the movement of an object, which is calculated following VBench [21].

**Compared Baselines.** In order to achieve unification of V2V tasks, which involve numerous tasks, we compare with specialized models for each task. For some tasks lacking open-source methods, we use commercially available online models as substitutes. The specific tasks can be divided into: (1) Repainting tasks, where in inpainting we mainly compare ProPainter [62] and the VACE 1.3B [23] task, and in outpainting, we mainly compare M3DDM [11] and the VACE 1.3B; (2) mask-guided video edit tasks, where we mainly compare Kling 1.6 [24] and VACE 1.3B [23]; (3) Instruction edit tasks, for which there are no corresponding open-source models, we mainly compare the commercial products Kling 1.6 and Pika [40]; (4) Character Animation tasks, where we mainly compare Animate Anyone [18], Mimicmotion [59], and Champ [64], and for Controllable Character Video Synthesis tasks, we mainly compare Mimo [37].

## 4.2 Main Results

**Qualitative Results.** To fully validate the superiority of our method, as shown in the figure 4, we conducted comparisons with existing approaches on tasks such as mask-guided editing and try-on. Our method achieves more realistic and temporally consistent results on the wild dataset compared to VACE 1.3B and Kling 1.6, with objects in the edited regions exhibiting more natural motion. Of course, qualitative comparisons for other tasks can be found in the supplementary materials. Moreover, our model can effectively integrate conditions from different modalities. As illustrated in the figure 5, we showcase the performance of our model across various sub-tasks, demonstrating its strong potential in the field of video generation and editing. More visualization results are available in the supplementary.



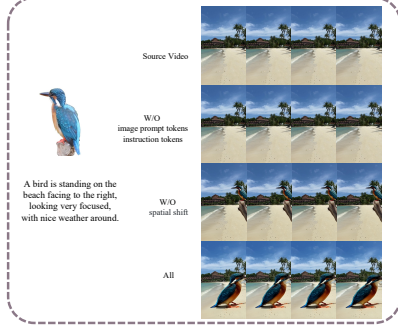


Figure 6: Ablation Study

Table 2: Ablation study on token fusion.

Task	Method	DINO-sim $\uparrow$	FVD $\downarrow$	Temporal $\uparrow$	DD $\uparrow$
(1)	w/o FC	0.544	1200.96	0.662	0.63
	w FC	<b>0.55</b>	<b>862.21</b>	<b>0.86</b>	<b>0.64</b>
(2)	w/o FC	0.548	980.49	0.942	0.57
	w FC	<b>0.59</b>	<b>900.35</b>	<b>0.97</b>	<b>0.69</b>

**Quantitative Results.** To further comprehensively validate the superiority of our method across various tasks, we conducted extensive comparisons with a range of task-specific approaches on our OmniV2V-Test. We mainly compare two relatively complex tasks: mask-guided video edit and controllable character video synthesis. As shown in table 1, our method achieves the best performance in terms of FVD, object consistency, temporal consistency, and dynamic degree. Although there is still a certain gap compared to the commercial model Kling 1.6 in Clip-B and Clip-L, our method performs on par with VACE 1.3B. Notably, compared to Keling 1.6 and VACE 1.3B, our model demonstrates clear advantages in object consistency and dynamic degree on the mask-guided video edit and try-on tasks. For quantitative comparison results on other tasks, please refer to supplementary.

**User Study** To further validate the effectiveness of our proposed method, we conducted evaluations on the objective assessment dataset of the OmniV2V-Test benchmark. Each participant assessed three key dimensions: Subject Consistency (SC), Motion Dynamic (MD), and Video Quality (VQ). A total of 30 participants scored each aspect on a scale from 0 to 10. As shown in the table 1, the results indicate that OmniV2V outperforms all existing baseline methods across all evaluated dimensions. Notably, it achieves particularly significant improvements in motion dynamic and object consistency. The evaluation clearly demonstrate the superiority of our approach.

### 4.3 Ablation Study And Discussion

**Ablation on token fusion.** The Table 2 demonstrates the effectiveness and necessity of the FC layer in the Token Fusion process for tasks such as (1) controllable character video synthesis, (2) mask-guided video editing. The FC layer effectively allows the model to selectively retain or discard features, ensuring that only the most salient conditional information is integrated.

**Ablation on posenet.** We evaluate how three different methods of injecting pose information affect the model’s ability to learn pose information. This evaluation is conducted on the controllable character video synthesis task. All three experiments are tested after 3000 training steps. As shown in the figure 7, injecting pose information using the token addition method leads to the model failing to properly understand the front and back of the character, making it unable to capture actions such as turning around. The controlnet-based method results in slow or even incorrect learning of character movements. Our method effectively addresses the issues present in the aforementioned approaches.

**Ablation on VLLM-driven instruction-based editing module.** In the Addition experiment, we validated the effectiveness of our VLLM-driven instruction-based editing module. As shown in the Figure 6, removing 3D-RoPE causes the model to simply copy and paste the image into the video, indicating that the spatial shift we introduced is effective. Additionally, the instruction tokens and image prompt tokens significantly aid the model in understanding the video content and performing relevant edits.

## 5 Conclusion

In this paper, we explore a unified dynamic content manipulation injection module that effectively integrates the requirements of various tasks. To enhance the model’s ability to understand the

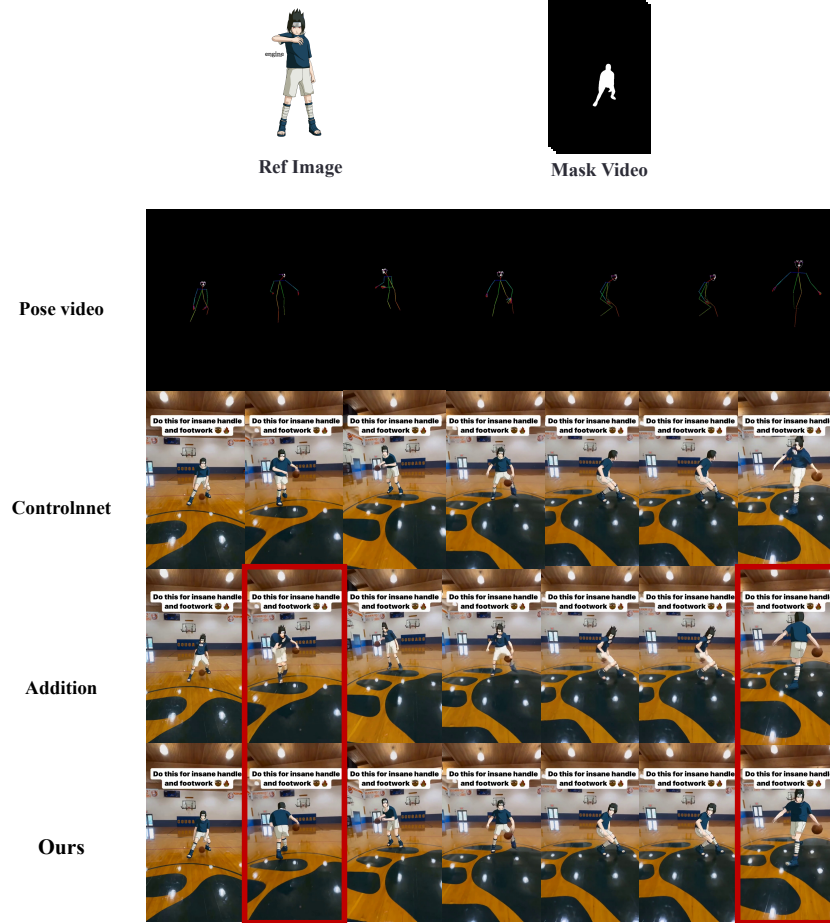


Figure 7: Ablation study on the posenet.

correspondence between visual content and text, we design a visual-text instruction module based on LLaVA. Given the numerous subtasks involved, we have developed a comprehensive multi-task data processing system. Since there is data overlap among various tasks, this system efficiently provides data augmentation. Using this system, we have constructed a multi-type, multi-scenario OmniV2V dataset, which significantly enhances the model’s capabilities. Additionally, we have developed the corresponding OmniV2V-Test benchmark. The extensive distribution of test data allows for a thorough evaluation of model performance across various tasks. Both qualitative and quantitative experiments demonstrate that OmniV2V shows significant improvements over the best current open-source and commercial models in various video generation and editing tasks.

## 6 Appendix

### 6.1 More visualization results

As shown in the figure 10 and figure 11, we present more visual results for the controllable character video synthesis task and mask-guided edit task. It can be seen that our method demonstrates strong generalization across various scenarios. Moreover, our model largely addresses the issue of object shape mismatch caused by mask boundaries.

As shown in the figure 12, we present more visual results for both inpainting and outpainting tasks. our model effectively identifies small and fast-moving objects and successfully removes them, demonstrating the model’s ability to handle complex scenarios with precision and efficiency. For the outpainting task, our model demonstrates the ability to generalize across various styles, such as anime

and traditional chinese painting. This versatility highlights the model’s adaptability and effectiveness in handling diverse artistic expressions.

As shown in figure 13, we provide additional visual results for the human animation and instruction edit tasks. In the human animation task, our method can accurately drive characters in various styles based on pose information, fully demonstrating the exceptional generalization capabilities of our approach. In the task of instruction edit, our method demonstrates impressive capabilities by directly replacing a bus in the video with a fire truck based on the given instructions, without the need for masking. This highlights the efficiency and precision of our approach in seamlessly handling complex video editing. Additionally, we showcase a scene where a woman is explaining cosmetics, illustrating the potential application of our model in the live streaming domain. By leveraging the capabilities of the model, users can easily modify visual elements to suit various backgrounds and themes, thereby expanding the creative horizons of digital media production.

## 6.2 More Experiments Results.

**More Qualitative Results.** As shown in the figure 9 and figure 11, our model achieves better results compared to both open-source and commercial methods in other tasks. Specifically, in the instruction addition task, our method is able to understand the information in the text while reducing the problem of the model faithfully replicating the original image. In the inpainting task, we found that the Kling1.6 [24] model always tries to modify content outside the mask, resulting in lower video quality. In the outpainting task, VACE1.3B [23] fails to generate boundary extensions that match the textual descriptions well. In the controllable character video synthesis task, we mainly compare with the open-source model Mimo [37]. It can be seen that our method achieves better subject similarity than Mimo.

**More Quantitative Results.** We present the quantitative comparison results for other tasks in table 3. For the **instruction addition** task, subjective evaluation shows that Pika pays insufficient attention to the positional information described in the text. However, it achieves the best performance on the motion dynamic (MD) metric, indicating high video dynamism, but its subject consistency (SC) score is relatively low, reflecting poor consistency. On the other hand, Kling1.6 [24], suffers from severe "hard-copy" issues. As shown in the table 3, Kling1.6 achieves excellent subject consistency, but its motion dynamics are extremely poor, suggesting that the model simply copies the input without understanding the relationship between text and image. Our model strikes a balance between dynamism and consistency, delivering higher video quality and outperforming both Kling1.6 and VACE1.3B [23] across all objective metrics. For the **human animation** task, our model significantly outperforms the open-source model MimicMotion [38] in all aspects. For the **inpaint** task, subjective evaluation indicates that Kling1.6 produces higher video quality. However, we found that this is mainly because Kling1.6 processes the input video at a higher resolution, resulting in better visual perception. VACE1.3B performs better in terms of dynamic degree(DD), which is mainly due to incomplete object removal during inpainting. On all other metrics, our model surpasses both Kling1.6 and VACE1.3B. For the **outpaint** task, alignment between text and video is particularly important. We observe that VACE1.3B performs poorly in text-video alignment, but achieves better video dynamics. This is because VACE1.3B tends to generate more variable content at the boundaries, leading to instability in the generated results.

## 6.3 Preliminary

Taking the controllable character video synthesis task as an example, we first resize the reference images  $I_1$  and  $I_2$  to match the dimensions of the target video. We then use the 3DVAE pretrained by HunyuanVideo13B to map the reference images  $I_1$  and  $I_2$  from the image space to the latent space, obtaining latent representations  $v_1$  and  $v_2$ , where  $w$  and  $h$  denote the width and height of the latent, and  $c$  is the feature dimension. These latents are then processed by Tokenizer1 to obtain  $t_1$  and  $t_2$ .

Similarly, the noise video, masked video, mask video, and pose video are passed through the 3DVAE to obtain  $v_{\text{noise}}$ ,  $v_{\text{md}}$ ,  $v_{\text{mv}}$ , and  $v_p$ , respectively. Next,  $v_R$  and  $v_{\text{noise}}$  are processed by Tokenizer1 ( $K_1$ ) to obtain  $t_R$  and  $t_{\text{noise}}$ . The features  $v_{\text{md}}$  and  $v_{\text{mv}}$  are concatenated along the channel dimension to form  $v_{\text{dv}}$ , which is then processed by Tokenizer2 ( $K_2$ , initialized with the weights of Tokenizer1) to obtain  $T_M$ . The pose feature  $v_p$  is processed by PoseNet and Tokenizer3 ( $K_3$ , also initialized with the weights of Tokenizer1) to obtain  $t_p$ .

Table 3: Quantitative comparisons with other tasks baselines.

Method	DINO-sim $\uparrow$	CLIP-B $\uparrow$	CLIP-L $\uparrow$	FVD $\downarrow$	Temporal $\uparrow$	DD $\uparrow$	SC $\uparrow$	MD $\uparrow$	VQ $\uparrow$
Kling1.6	0.543	0.308	0.265	1055.88	0.812	0.546	<b>7.50</b>	2.88	3.38
Pika	0.588	0.313	0.268	997.45	0.837	0.662	6.67	<b>5.77</b>	6.99
Ours	<b>0.596</b>	<b>0.321</b>	<b>0.268</b>	<b>968.74</b>	<b>0.854</b>	<b>0.766</b>	6.98	4.78	<b>7.32</b>
Mimicmotion	0.426	–	–	1210.70	0.823	0.842	3.88	4.32	6.66
Ours	<b>0.587</b>	–	–	<b>998.04</b>	<b>0.964</b>	<b>0.849</b>	<b>5.48</b>	<b>6.69</b>	<b>8.84</b>
Kling1.6	–	–	–	1200.56	0.754	0.664	7.98	7.14	<b>7.66</b>
VACE1.3B	–	–	–	960.21	0.815	<b>0.688</b>	7.68	7.00	6.43
Ours	–	–	–	<b>942.38</b>	<b>0.856</b>	0.669	<b>8.23</b>	<b>7.65</b>	7.55
VACE1.3B	–	<b>0.342</b>	<b>0.284</b>	1122.56	0.804	0.556	6.98	5.74	8.64
Ours	–	0.338	0.272	<b>984.24</b>	<b>0.841</b>	<b>0.643</b>	<b>7.02</b>	<b>7.65</b>	<b>8.82</b>

We then sum  $t_{\text{noise}}$ ,  $t_p$ , and  $T_M$ , and concatenate the result with  $t_1$  and  $t_2$  along the token dimension, together with  $t_R$ , to obtain the final input  $H$ , as shown in the following equation:

$$H = \text{TokenCat}(t_1, t_2, \{K_2(v_{\text{dv}}) + K_1(v_{\text{noise}}) + K_3(v_p)\}) \quad (2)$$

In the training process, we adopt the Flow Matching [34] framework to train the video generation models. For training, we first acquire the video latent representation  $z_1$  and the corresponding identity image  $I$ . Then, we sample  $t \in [0, 1]$  from a logit-normal distribution [10] and initialize the noise  $z_0 \sim N(0, I)$  according to the Gaussian distribution. After that, we construct the training sample  $z_t$  through linear interpolation. The model aims to predict the velocity  $u_t = \frac{dz_t}{dt}$  conditioned on the target image  $I$ , which is used to guide the sample  $z_t$  towards  $z_1$ . The model parameters are optimized by minimizing the mean-squared error between the predicted velocity  $v_t$  and the real velocity  $u_t$ , and the loss function is defined as:

$$\mathcal{L}_{\text{generation}} = \mathbb{E}_{t, x_0, x_1} \|v_t - u_t\|^2. \quad (3)$$

To endow our model with a more extensive representational capacity and enable it to capture and learn a broader range of complex patterns, we fully fine-tune the weights of both the pretrained video generation model and the LLaVA model, ultimately unlocking its full potential for delivering superior video customization results.

## 6.4 Implementation Details

During training, we initialize the model with the weights of HunyuanVideo13B [28], and keep the parameters of LLaVA and 3DVAE frozen, updating only all other parameters. The training is divided into two stages: in the first stage, we use 128 GPUs (each with 96GB memory), set the training video resolution to 540×896, the global batch size to 64, and the learning rate to 1e-5, training for 10,000 steps; in the second stage, we use 256 GPUs (each with 96GB memory), set the training video resolution to 720×1280, the global batch size to 128, and the learning rate to 3e-5, training for 20,000 steps.

## 6.5 Limitations and Societal Impacts

**Limitations** Our method demonstrates strong capabilities across various video-to-video tasks. However, since the instruction edit task is primarily driven by text input, this signal is relatively weaker compared to signals such as mask or pose. As a result, there are scenarios where the instruction signal is ineffective. For example, when replacing very small objects (such as insects), the model may fail to accurately identify and replace the target object.

Meanwhile, in the controllable character video synthesis task, we observe that issues related to character interaction caused by mask boundaries still occur frequently. For instance, when replacing a person holding a spear with a person holding a golden staff, the model often fails to generate the hands properly, resulting in poor interaction between the character and the object.

**Societal impacts** As intelligent video generation and editing technologies become increasingly widespread, society is also facing new challenges. The convenience of generating and editing video content may lead to the spread of misinformation and false content, undermining public trust in information. At the same time, these technologies may inadvertently reinforce existing biases and stereotypes during content creation, negatively impacting cultural perceptions within society. These issues have sparked deep reflection on ethics and responsibility, prompting policymakers, technology developers, and all sectors of society to work together to establish appropriate regulations to ensure the healthy development of these technologies. We should also approach their potential impacts with caution, actively seeking a balance between innovation and social responsibility so that these technologies can bring greater benefits to society.

On the positive side, intelligent video generation and editing provide creators with a wealth of innovative tools, inspiring new ideas and enhancing the artistic and creative quality of video content. These technologies are gradually permeating various industries. For example, in the business sector, video generation technology is revolutionizing marketing and advertising strategies. Companies can quickly produce high-quality promotional videos, effectively communicate brand messages, and attract more consumers. This increase in efficiency not only reduces labor costs but also enables businesses to implement more creative marketing campaigns, thereby strengthening their competitiveness in the market.

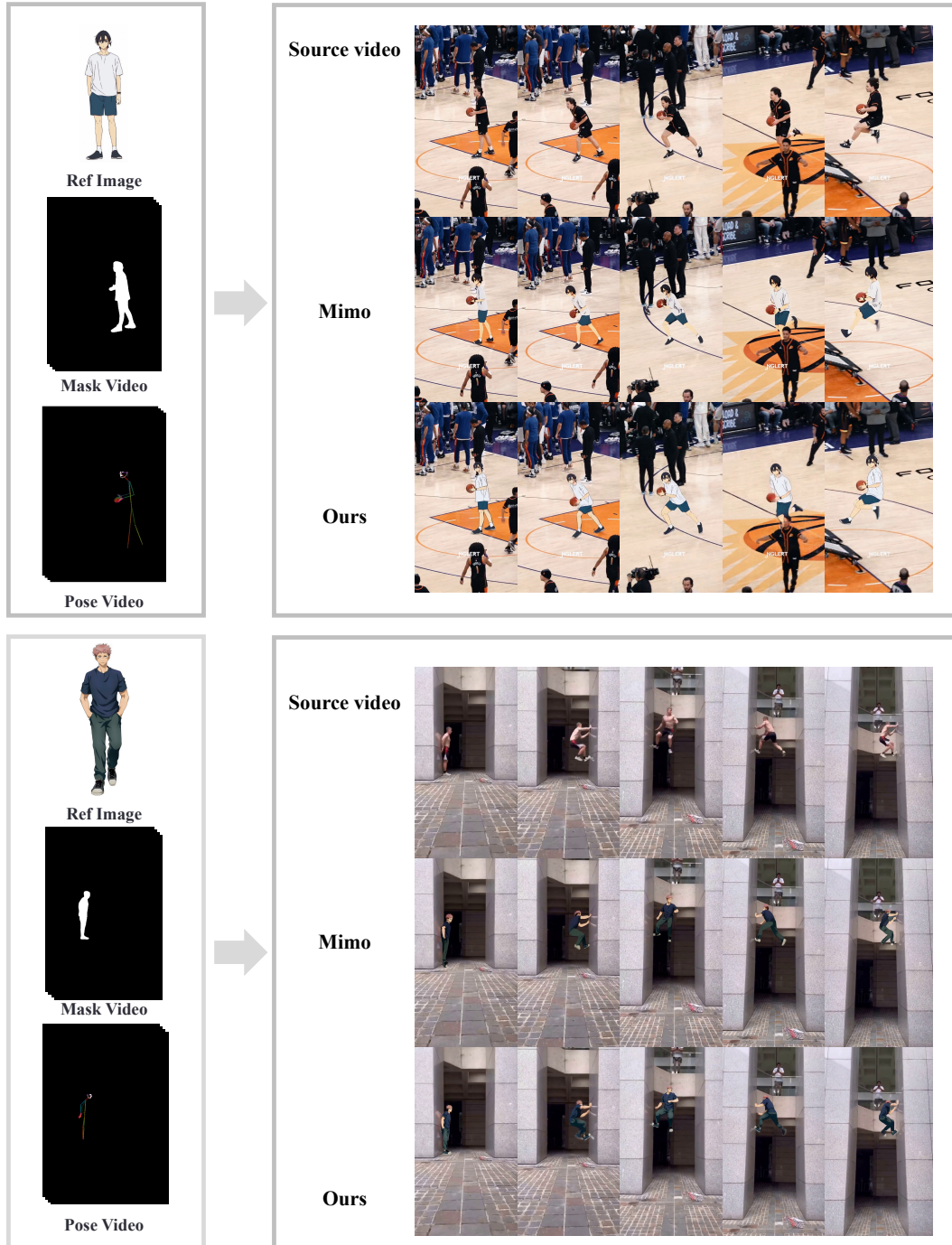


Figure 8: Qualitative comparison with MIMO on the controllable character video synthesis task.



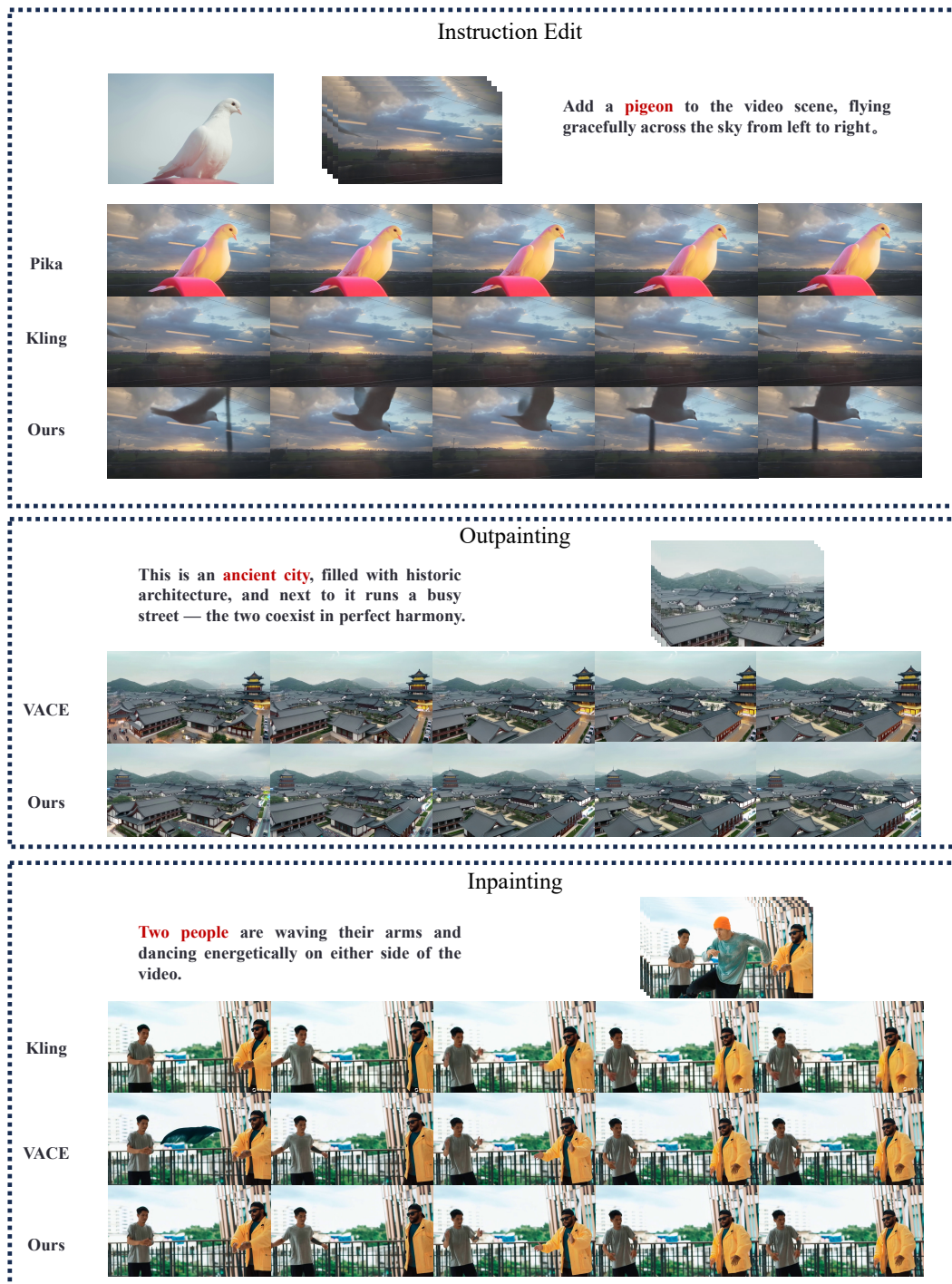
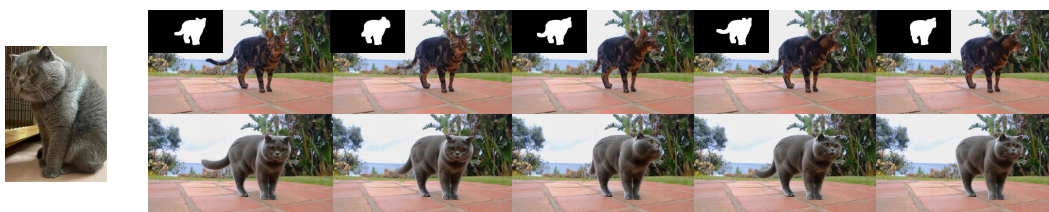
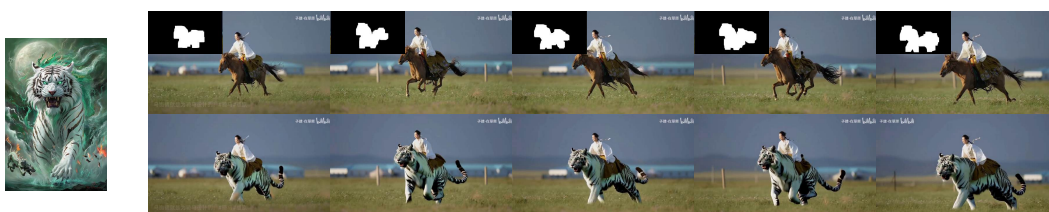


Figure 9: Qualitative of comparison on instruction edit, outpainting and inpainting task.

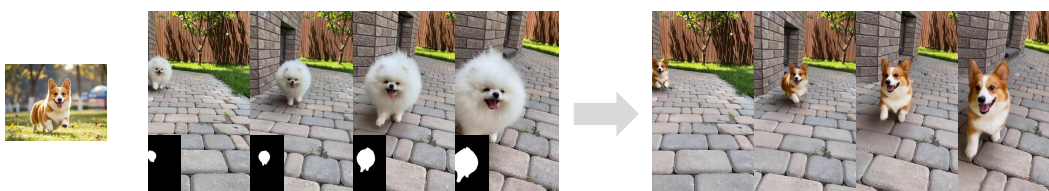
A gray British Shorthair cat with round eyes stands on the ground paved with reddish-brown bricks.



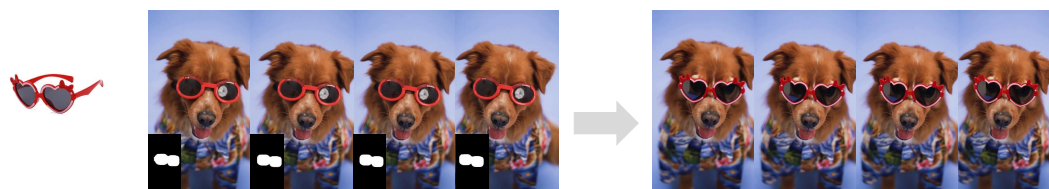
A girl is riding a white tiger running across the meadow.



A joyful brown Corgi bounds towards the camera with enthusiasm from afar.



A brown dog is wearing a pair of red heart-shaped glasses.



A blue jay (Cyanocitta cristata) is eating the food in a person's hand and then flies away.



A is playing a red guitar with a sharp body shape, and there are snow-capped mountains in the background.

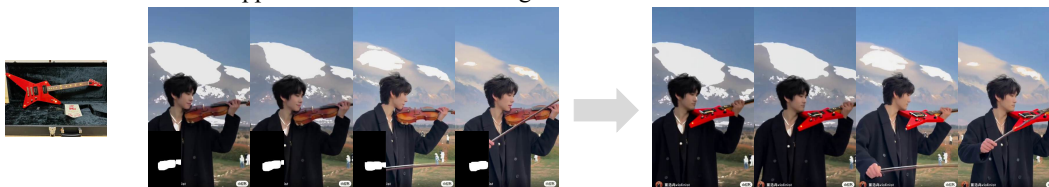


Figure 10: More visualizations of mask-guided edit task.



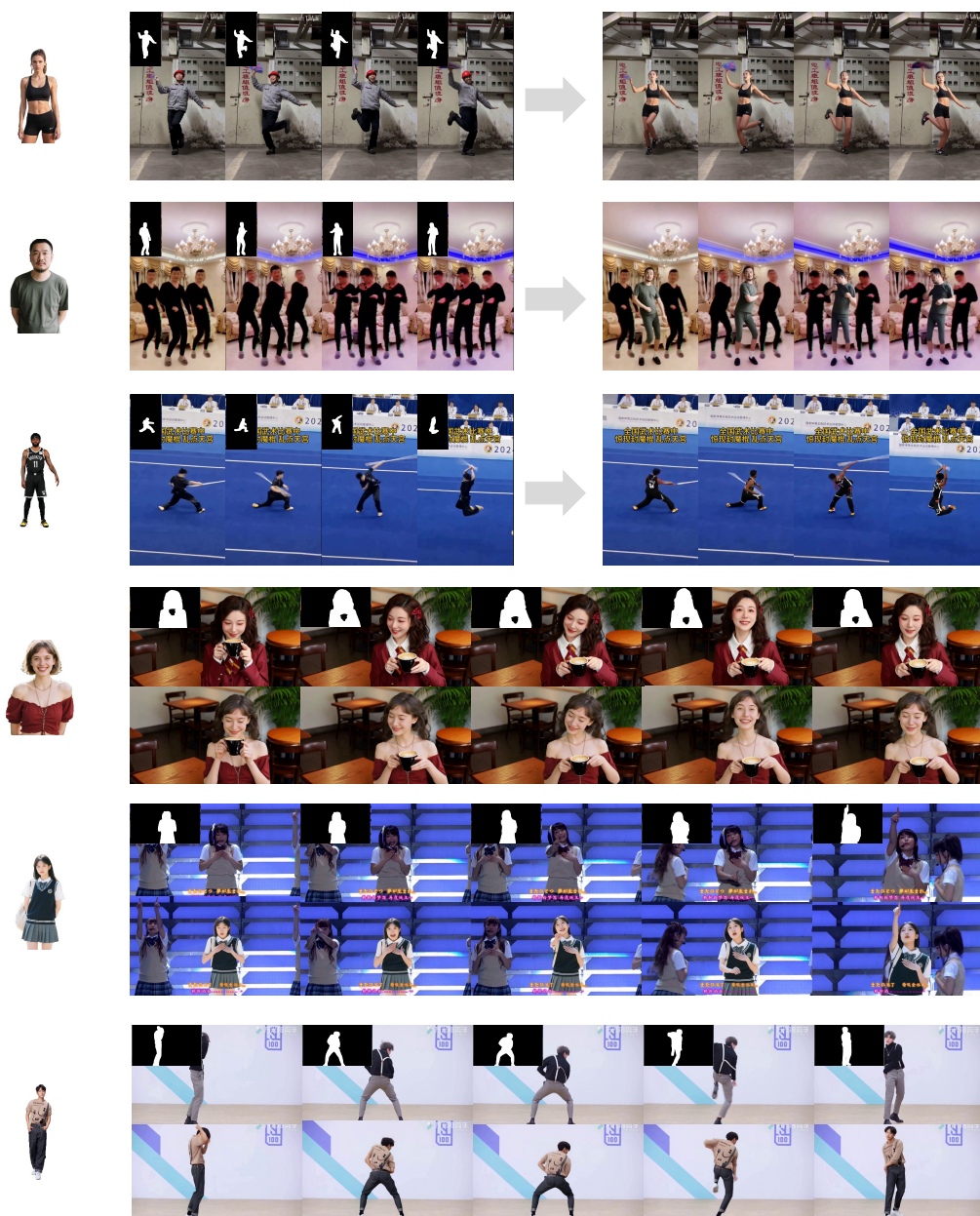


Figure 11: More visualizations of controllable character video synthesis task.

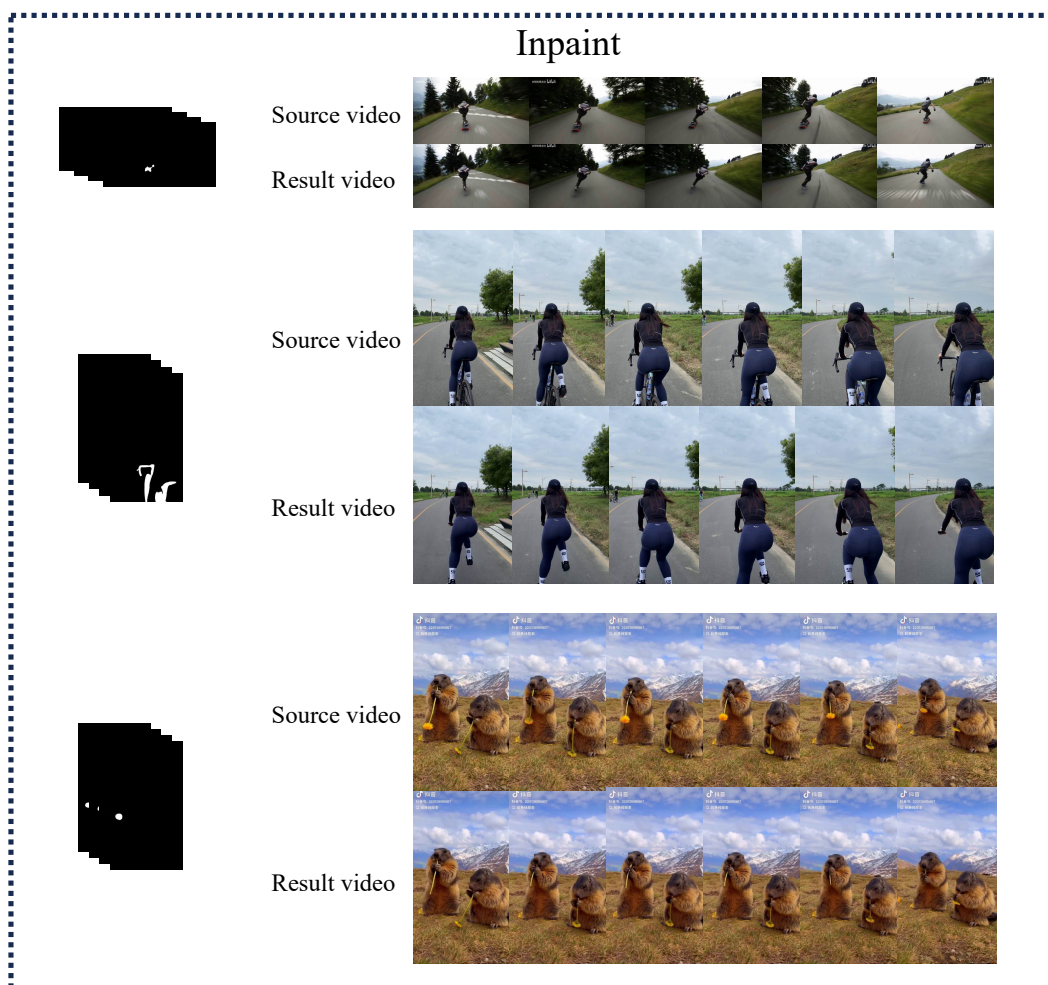
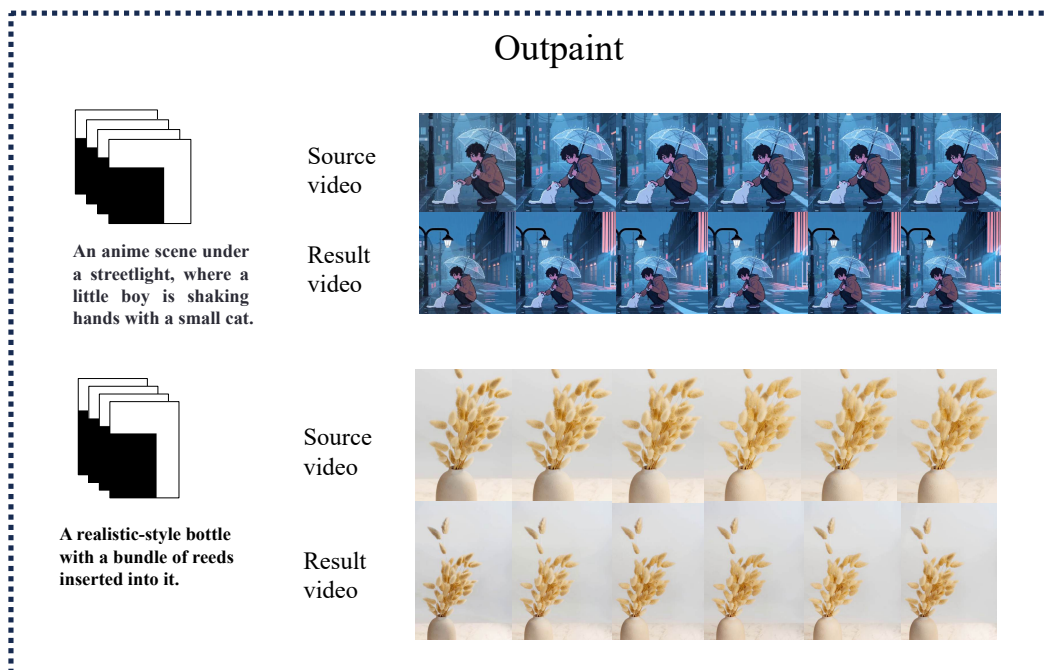


Figure 12: More visualizations of outpainting and inpainting task.

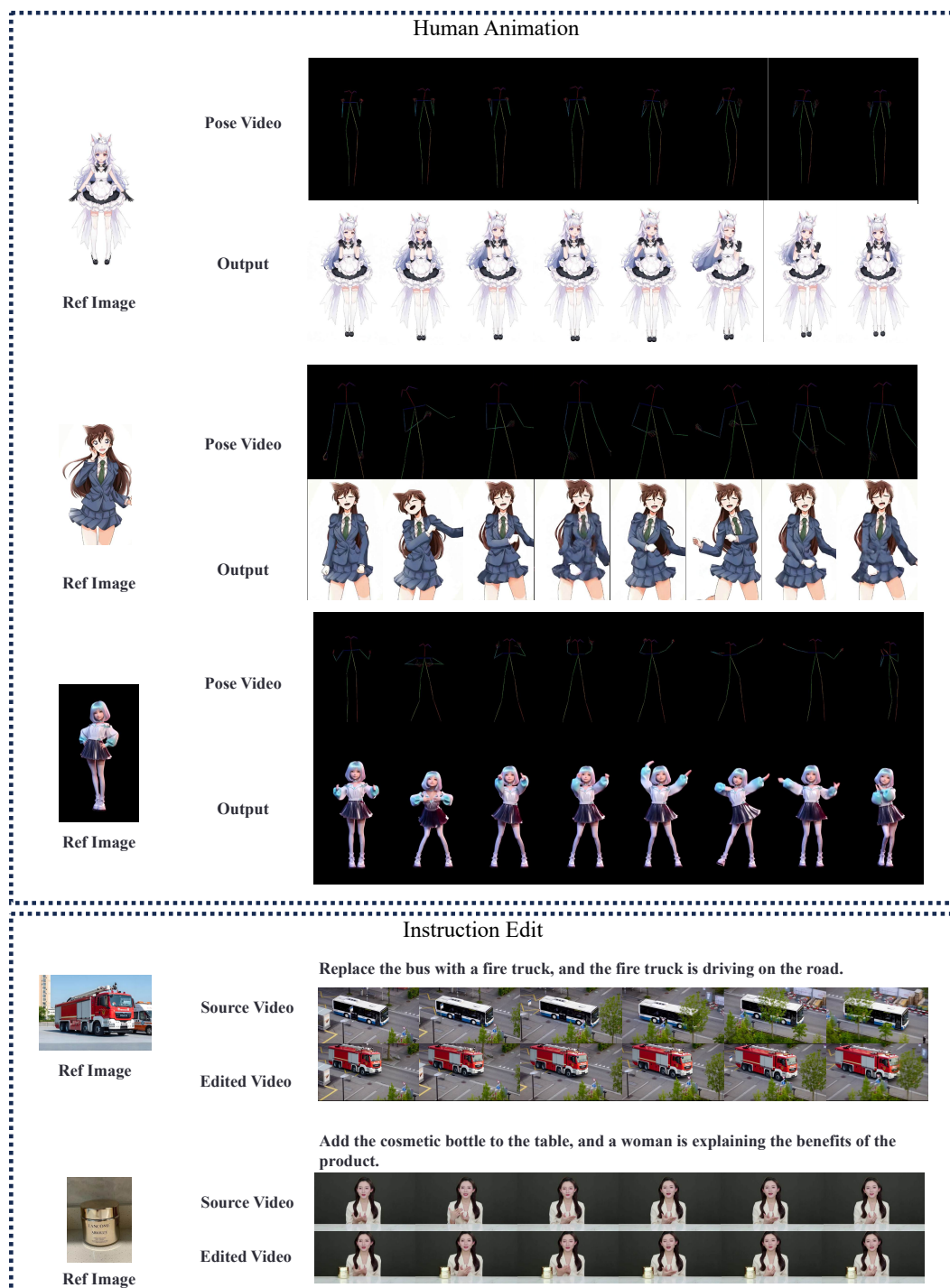


Figure 13: More visualizations of human animation and instruction edit task.

## References

- [1] J. Bai, S. Bai, Y. Chu, Z. Cui, K. Dang, X. Deng, Y. Fan, W. Ge, Y. Han, F. Huang, et al. Qwen technical report. *arXiv preprint arXiv:2309.16609*, 2023.
- [2] O. Bar-Tal, H. Chefer, O. Tov, C. Herrmann, R. Paiss, S. Zada, A. Ephrat, J. Hur, Y. Li, T. Michaeli, et al. Lumiere: A space-time diffusion model for video generation. *arXiv preprint arXiv:2401.12945*, 2024.
- [3] Y. Bian, Z. Zhang, X. Ju, M. Cao, L. Xie, Y. Shan, and Q. Xu. Videopainter: Any-length video inpainting and editing with plug-and-play context control. *arXiv preprint arXiv:2503.05639*, 2025.
- [4] A. Blattmann, T. Dockhorn, S. Kulal, D. Mendelevitch, M. Kilian, D. Lorenz, Y. Levi, Z. English, V. Voleti, A. Letts, et al. Stable video diffusion: Scaling latent video diffusion models to large datasets. *arXiv preprint arXiv:2311.15127*, 2023.
- [5] A. Blattmann, R. Rombach, H. Ling, T. Dockhorn, S. W. Kim, S. Fidler, and K. Kreis. Align your latents: High-resolution video synthesis with latent diffusion models. In *Proceedings of the IEEE/CVF Conference on Computer Vision and Pattern Recognition*, pages 22563–22575, 2023.
- [6] T. Brooks, J. Hellsten, M. Aittala, T.-C. Wang, T. Aila, J. Lehtinen, M.-Y. Liu, A. Efros, and T. Karras. Generating long videos of dynamic scenes. *Advances in Neural Information Processing Systems*, 35:31769–31781, 2022.
- [7] H. W. Chung, L. Hou, S. Longpre, B. Zoph, Y. Tay, W. Fedus, Y. Li, X. Wang, M. Dehghani, S. Brahma, et al. Scaling instruction-finetuned language models. *Journal of Machine Learning Research*, 25(70):1–53, 2024.
- [8] J. Deng, J. Guo, N. Xue, and S. Zafeiriou. Arcface: Additive angular margin loss for deep face recognition. In *Proceedings of the IEEE/CVF conference on computer vision and pattern recognition*, pages 4690–4699, 2019.
- [9] J. Deng, J. Guo, E. Ververas, I. Kotsia, and S. Zafeiriou. Retinaface: Single-shot multi-level face localisation in the wild. In *CVPR*, 2020.
- [10] P. Esser, S. Kulal, A. Blattmann, R. Entezari, J. Müller, H. Saini, Y. Levi, D. Lorenz, A. Sauer, F. Boesel, et al. Scaling rectified flow transformers for high-resolution image synthesis. In *Forty-first international conference on machine learning*, 2024.
- [11] F. Fan, C. Guo, L. Gong, B. Wang, T. Ge, Y. Jiang, C. Luo, and J. Zhan. Hierarchical masked 3d diffusion model for video outpainting. In *Proceedings of the 31st ACM International Conference on Multimedia*, pages 7890–7900, 2023.
- [12] Z. Fang, W. Zhai, A. Su, H. Song, K. Zhu, M. Wang, Y. Chen, Z. Liu, Y. Cao, and Z.-J. Zha. Vivid: Video virtual try-on using diffusion models. *arXiv preprint arXiv:2405.11794*, 2024.
- [13] Y. Gao, Y. Zhou, J. Wang, X. Li, X. Ming, and Y. Lu. High-fidelity and freely controllable talking head video generation. In *Proceedings of the IEEE/CVF conference on computer vision and pattern recognition*, pages 5609–5619, 2023.
- [14] Y. Guo, C. Yang, A. Rao, Z. Liang, Y. Wang, Y. Qiao, M. Agrawala, D. Lin, and B. Dai. Animatediff: Animate your personalized text-to-image diffusion models without specific tuning. *arXiv preprint arXiv:2307.04725*, 2023.
- [15] A. Gupta, L. Yu, K. Sohn, X. Gu, M. Hahn, L. Fei-Fei, I. Essa, L. Jiang, and J. Lezama. Photorealistic video generation with diffusion models. *arXiv preprint arXiv:2312.06662*, 2023.
- [16] J. Ho, T. Salimans, A. Gritsenko, W. Chan, M. Norouzi, and D. J. Fleet. Video diffusion models. *Advances in Neural Information Processing Systems*, 35:8633–8646, 2022.
- [17] W. Hong, M. Ding, W. Zheng, X. Liu, and J. Tang. Cogvideo: Large-scale pretraining for text-to-video generation via transformers. *arXiv preprint arXiv:2205.15868*, 2022.



- [18] L. Hu. Animate anyone: Consistent and controllable image-to-video synthesis for character animation. In *Proceedings of the IEEE/CVF Conference on Computer Vision and Pattern Recognition*, pages 8153–8163, 2024.
- [19] L. Hu, G. Wang, Z. Shen, X. Gao, D. Meng, L. Zhuo, P. Zhang, B. Zhang, and L. Bo. Animate anyone 2: High-fidelity character image animation with environment affordance. *arXiv preprint arXiv:2502.06145*, 2025.
- [20] T. Hu, Z. Yu, Z. Zhou, S. Liang, Y. Zhou, Q. Lin, and Q. Lu. Hunyuancustom: A multimodal-driven architecture for customized video generation, 2025. URL <https://arxiv.org/abs/2505.04512>.
- [21] Z. Huang, Y. He, J. Yu, F. Zhang, C. Si, Y. Jiang, Y. Zhang, T. Wu, Q. Jin, N. Chanpaisit, et al. Vbench: Comprehensive benchmark suite for video generative models. In *Proceedings of the IEEE/CVF Conference on Computer Vision and Pattern Recognition*, pages 21807–21818, 2024.
- [22] J. Jiang, T. Wang, H. Yan, and J. Liu. Clothformer: Taming video virtual try-on in all module. In *Proceedings of the IEEE/CVF Conference on Computer Vision and Pattern Recognition*, pages 10799–10808, 2022.
- [23] Z. Jiang, Z. Han, C. Mao, J. Zhang, Y. Pan, and Y. Liu. Vace: All-in-one video creation and editing. *arXiv preprint arXiv:2503.07598*, 2025.
- [24] Keling. Keling. <https://klingai.com/cn/>, 2025.
- [25] R. Khanam and M. Hussain. Yolov11: An overview of the key architectural enhancements. *arXiv preprint arXiv:2410.17725*, 2024.
- [26] J. Kim, G. Gu, M. Park, S. Park, and J. Choo. Stableviton: Learning semantic correspondence with latent diffusion model for virtual try-on. In *Proceedings of the IEEE/CVF conference on computer vision and pattern recognition*, pages 8176–8185, 2024.
- [27] W. Kong, Q. Tian, Z. Zhang, R. Min, Z. Dai, J. Zhou, J. Xiong, X. Li, B. Wu, J. Zhang, et al. Hunyuanvideo: A systematic framework for large video generative models. *arXiv preprint arXiv:2412.03603*, 2024.
- [28] W. Kong, Q. Tian, Z. Zhang, R. Min, Z. Dai, J. Zhou, J. Xiong, X. Li, B. Wu, J. Zhang, et al. Hunyuanvideo: A systematic framework for large video generative models. *arXiv preprint arXiv:2412.03603*, 2024.
- [29] B. F. Labs. Flux. <https://github.com/black-forest-labs/flux>, 2024.
- [30] Y. Li, M. Min, D. Shen, D. Carlson, and L. Carin. Video generation from text. In *Proceedings of the AAAI conference on artificial intelligence*, volume 32, 2018.
- [31] Z. Li, J. Zhang, Q. Lin, J. Xiong, Y. Long, X. Deng, Y. Zhang, X. Liu, M. Huang, Z. Xiao, et al. Hunyuan-dit: A powerful multi-resolution diffusion transformer with fine-grained chinese understanding. *arXiv preprint arXiv:2405.08748*, 2024.
- [32] S. Lin, X. Xia, Y. Ren, C. Yang, X. Xiao, and L. Jiang. Diffusion adversarial post-training for one-step video generation. *arXiv preprint arXiv:2501.08316*, 2025.
- [33] Y. Lin, H. Fung, J. Xu, Z. Ren, A. S. Lau, G. Yin, and X. Li. Mvportrait: Text-guided motion and emotion control for multi-view vivid portrait animation. *arXiv preprint arXiv:2503.19383*, 2025.
- [34] Y. Lipman, R. T. Chen, H. Ben-Hamu, M. Nickel, and M. Le. Flow matching for generative modeling. *arXiv preprint arXiv:2210.02747*, 2022.
- [35] H. Liu, C. Li, Q. Wu, and Y. J. Lee. Visual instruction tuning. *Advances in neural information processing systems*, 36:34892–34916, 2023.

- [36] Y. Liu, K. Zhang, Y. Li, Z. Yan, C. Gao, R. Chen, Z. Yuan, Y. Huang, H. Sun, J. Gao, et al. Sora: A review on background, technology, limitations, and opportunities of large vision models. *arXiv preprint arXiv:2402.17177*, 2024.
- [37] Y. Men, Y. Yao, M. Cui, and L. Bo. Mimo: Controllable character video synthesis with spatial decomposed modeling. *arXiv preprint arXiv:2409.16160*, 2024.
- [38] R. Meng, X. Zhang, Y. Li, and C. Ma. Echomimicv2: Towards striking, simplified, and semi-body human animation. *arXiv preprint arXiv:2411.10061*, 2024.
- [39] M. Oquab, T. Darcet, T. Moutakanni, H. Vo, M. Szafraniec, V. Khalidov, P. Fernandez, D. Haziza, F. Massa, A. El-Nouby, et al. Dinov2: Learning robust visual features without supervision. *arXiv preprint arXiv:2304.07193*, 2023.
- [40] Pika. Pika. <https://pika.art/>, 2025.
- [41] PySceneDetect. Pyscenedetect. <https://github.com/Breakthrough/PySceneDetect>, 2025.
- [42] A. Radford, J. W. Kim, C. Hallacy, A. Ramesh, G. Goh, S. Agarwal, G. Sastry, A. Askell, P. Mishkin, J. Clark, et al. Learning transferable visual models from natural language supervision. In *International conference on machine learning*, pages 8748–8763. PmLR, 2021.
- [43] T. Ren, S. Liu, A. Zeng, J. Lin, K. Li, H. Cao, J. Chen, X. Huang, Y. Chen, F. Yan, Z. Zeng, H. Zhang, F. Li, J. Yang, H. Li, Q. Jiang, and L. Zhang. Grounded sam: Assembling open-world models for diverse visual tasks, 2024.
- [44] R. Rombach, A. Blattmann, D. Lorenz, P. Esser, and B. Ommer. High-resolution image synthesis with latent diffusion models. In *Proceedings of the IEEE/CVF conference on computer vision and pattern recognition*, pages 10684–10695, 2022.
- [45] U. Singer, A. Polyak, T. Hayes, X. Yin, J. An, S. Zhang, Q. Hu, H. Yang, O. Ashual, O. Gafni, et al. Make-a-video: Text-to-video generation without text-video data. *arXiv preprint arXiv:2209.14792*, 2022.
- [46] Y. Tu, H. Luo, X. Chen, S. Ji, X. Bai, and H. Zhao. Videoanydoor: High-fidelity video object insertion with precise motion control. *arXiv preprint arXiv:2501.01427*, 2025.
- [47] R. Villegas, M. Babaeizadeh, P.-J. Kindermans, H. Moraldo, H. Zhang, M. T. Saffar, S. Castro, J. Kunze, and D. Erhan. Phenaki: Variable length video generation from open domain textual descriptions. In *International Conference on Learning Representations*, 2022.
- [48] A. Wang, B. Ai, B. Wen, C. Mao, C.-W. Xie, D. Chen, F. Yu, H. Zhao, J. Yang, J. Zeng, et al. Wan: Open and advanced large-scale video generative models. *arXiv preprint arXiv:2503.20314*, 2025.
- [49] J. Wang, H. Yuan, D. Chen, Y. Zhang, X. Wang, and S. Zhang. Modelscope text-to-video technical report. *arXiv preprint arXiv:2308.06571*, 2023.
- [50] Q. Wang, Y. Shi, J. Ou, R. Chen, K. Lin, J. Wang, B. Jiang, H. Yang, M. Zheng, X. Tao, et al. Koala-36m: A large-scale video dataset improving consistency between fine-grained conditions and video content. *arXiv preprint arXiv:2410.08260*, 2024.
- [51] Y. Wang, P. Bilinski, F. Bremond, and A. Dantcheva. Imaginator: Conditional spatio-temporal gan for video generation. In *Proceedings of the IEEE/CVF Winter Conference on Applications of Computer Vision*, pages 1160–1169, 2020.
- [52] Z. Xu, M. Chen, Z. Wang, L. Xing, Z. Zhai, N. Sang, J. Lan, S. Xiao, and C. Gao. Tunnel try-on: Excavating spatial-temporal tunnels for high-quality virtual try-on in videos. In *Proceedings of the 32nd ACM International Conference on Multimedia*, pages 3199–3208, 2024.
- [53] Z. Xu, Z. Yu, Z. Zhou, J. Zhou, X. Jin, F.-T. Hong, X. Ji, J. Zhu, C. Cai, S. Tang, et al. Hunyuanportrait: Implicit condition control for enhanced portrait animation. *arXiv preprint arXiv:2503.18860*, 2025.

- [54] Z. Yang, A. Zeng, C. Yuan, and Y. Li. Effective whole-body pose estimation with two-stages distillation. In *Proceedings of the IEEE/CVF International Conference on Computer Vision*, pages 4210–4220, 2023.
- [55] Z. Yang, J. Teng, W. Zheng, M. Ding, S. Huang, J. Xu, Y. Yang, W. Hong, X. Zhang, G. Feng, et al. Cogvideox: Text-to-video diffusion models with an expert transformer. *arXiv preprint arXiv:2408.06072*, 2024.
- [56] L. Zhang, A. Rao, and M. Agrawala. Adding conditional control to text-to-image diffusion models. In *Proceedings of the IEEE/CVF International Conference on Computer Vision*, 2023.
- [57] S. Zhang, J. Wang, Y. Zhang, K. Zhao, H. Yuan, Z. Qin, X. Wang, D. Zhao, and J. Zhou. I2vgen-xl: High-quality image-to-video synthesis via cascaded diffusion models. *arXiv preprint arXiv:2311.04145*, 2023.
- [58] S.-X. Zhang, C. Yang, X. Zhu, and X.-C. Yin. Arbitrary shape text detection via boundary transformer. *IEEE Transactions on Multimedia*, 2023.
- [59] Y. Zhang, J. Gu, L.-W. Wang, H. Wang, J. Cheng, Y. Zhu, and F. Zou. Mimicmotion: High-quality human motion video generation with confidence-aware pose guidance. *arXiv preprint arXiv:2406.19680*, 2024.
- [60] X. Zhong, Z. Wu, T. Tan, G. Lin, and Q. Wu. Mv-ton: Memory-based video virtual try-on network. In *Proceedings of the 29th ACM International Conference on Multimedia*, pages 908–916, 2021.
- [61] D. Zhou, W. Wang, H. Yan, W. Lv, Y. Zhu, and J. Feng. Magicvideo: Efficient video generation with latent diffusion models. *arXiv preprint arXiv:2211.11018*, 2022.
- [62] S. Zhou, C. Li, K. C. Chan, and C. C. Loy. Propainter: Improving propagation and transformer for video inpainting. In *Proceedings of the IEEE/CVF international conference on computer vision*, pages 10477–10486, 2023.
- [63] Y. Zhou, Q. Wang, Y. Cai, and H. Yang. Allegro: Open the black box of commercial-level video generation model. *arXiv preprint arXiv:2410.15458*, 2024.
- [64] S. Zhu, J. L. Chen, Z. Dai, Y. Xu, X. Cao, Y. Yao, H. Zhu, and S. Zhu. Champ: Controllable and consistent human image animation with 3d parametric guidance. In *European Conference on Computer Vision (ECCV)*, 2024.
- [65] S. Zhuang, Z. Huang, B. Yang, Y. Zhang, F. Wang, C. Fu, C. Sun, Z.-J. Zha, C. Li, and Y. Wang. Get in video: Add anything you want to the video. *arXiv preprint arXiv:2503.06268*, 2025.
- [66] B. Zi, S. Zhao, X. Qi, J. Wang, Y. Shi, Q. Chen, B. Liang, R. Xiao, K.-F. Wong, and L. Zhang. Cococo: Improving text-guided video inpainting for better consistency, controllability and compatibility. In *Proceedings of the AAAI Conference on Artificial Intelligence*, volume 39, pages 11067–11076, 2025.